Propellants,
Explosives,
Pyrotechnics

DOI: 10.1002/prep.201500151

Synthesis and Degradation of Hexamethylene Triperoxide Diamine (HMTD)

Jimmie C. Oxley,*[a] James L. Smith,[a] Matthew Porter,[a] Lindsay McLennan,[a] Kevin Colizza,[a] Yehuda Zeiri,[b, c] Ronnie Kosloff,[d] and Faina Dubnikova[d]

Abstract: The synthesis and decomposition of hexamethylene triperoxide diamine (HMTD) were studied. Mechanisms were proposed based on isotopic labeling and mass spectral interpretation of both condensed phase products and head-space products. Formation of HMTD from hexamine appeared to proceed from dissociated hexamine as evident from scrambling of the ^{15}N label when synthesis was carried out with equal molar labeled/unlabeled hexamine. Decomposition of HMTD was considered with additives and in the presence and absence of moisture. In addition to mass spectral interpretation, density functional theory (DFT) was used to calculate energy differences of transition states and the entropies of intermediates along different possible decomposition pathways. HMTD is destabilized by water and citric acid making purification following initial synthesis essential in order to avoid unanticipated violent reaction.

Keywords: Hexamethylene triperoxide diamine (HMTD) · Synthesis · Decomposition mechanisms · Isotopic labels · Head-space products

1 Introduction

HMTD is synthesized from the reaction of hexamine with hydrogen peroxide. The oxidation is catalyzed by acid, usually citric acid. It was discovered in 1885 by Legler using formaldehyde, ammonium sulfate, and hydrogen peroxide [1]. The structure was proposed in 1900 by Baeyer and Villiger [2]. Von Girsewald was the first to use hexamine, citric acid, and hydrogen peroxide [3]. X-ray diffraction showed exactly planar threefold coordination about the two bridgehead nitrogen atoms rather than pyramidal structure [4,5]. This ring strain in HMTD may account for its low thermal stability and high sensitivity to friction [6,7]. Because there have been several unexpected violent reactions involving HMTD where counterterrorism personnel have been injured, we launched a study to better understand its chemistry and, for the purposes of detection, to identify its signature under a variety of conditions.

2 Experimental Section

2.1 Synthesis of HMTD with Citric Acid

HMTD was synthesized according to the literature [5]. The yield of crude HMTD was ca. 50%, assuming 1:1 molar ratio hexamine:HMTD. Recrystallization was conducted with 70/30 v/v mix of ethyl acetate (EA)/acetonitrile (ACN). Solvent was difficult to remove even after drying under high vacuum for 24 h. The evidence collected to support that HMTD was synthesized with these conditions included GC/MS (see Section 2.12), DSC (see Section 2.10), melting point (by Mel-Temp apparatus), LC/MS (see Section 2.14), NMR (Bruker 300 MHz, ^{1}H NMR [$CDCl_3$]: $\delta = 4.80$), and IR (Thermo Nicolet 6700 FTIR). The evidence gathered to support that HMTD was synthesized under any of the alternate conditions listed below (including labeling studies) included GC/MS, melting point, and LC/MS.

Note: HMTD is an extremely sensitive primary explosive; no fritted glass, metal spatulas nor excess force or friction should be applied.

2.2 Synthesis of HMTD with Other Acids or No Acid

Using same amounts of hexamine and hydrogen peroxide as above, but no acid added, precipitation of HMTD was

---

[a] J. C. Oxley, J. L. Smith, M. Porter, L. McLennan, K. Colizza
Department of Chemistry
University of Rhode Island
Kingston, RI, USA 02881
*e-mail: joxley@chm.uri.edu

[b] Y. Zeiri
Biomedical Engineering
Ben-Gurion University
Beer-Sheva, 84105 Israel

[c] Y. Zeiri
Department of Chemistry
NRCN P. O. Box 9001
Beer-Sheva, 84190, Israel

[d] R. Kosloff, F. Dubnikova
Department of Chemistry
Hebrew University
Jerusalem, Israel

not observed for 7 d at room temperature. After 9 d of stirring, 261 mg HMTD was recovered, ca. 7% yield assuming 1:1 molar ratio hexamine:HMTD. Other diprotic and triprotic acids used, in place of citric acid, included sulfuric acid, phosphoric acid, and oxalic acid; like citric acid, they were added in 1.1 to 1 molar ratios hexamine:acid. Monoprotic acids gave poor yields (Table 5) if added in 1.1 to 1 molar ratios. If these (acetic acid, trifluoroacetic acid, formic acid, and nitric acid) were added in a 2.2 to 1 molar ratio hexamine:acid, yields were comparable to those achieved with citric acid.

2.3 Synthesis of HMTD with Formaldehyde (^{13}C or ^{12}C)

Formaldehyde, up to 6 mol per mole hexamine, appeared to accelerate the reaction and increased the yield to over 100% based 1 to 1 hexamine:HMTD. For example, HMTD was synthesized by adding hexamine (0.4499 g, 3.22 mmol) to a solution of ^{13}C formaldehyde in water (2.0153 g of solution, 20 wt%, 13.43 mmol) in an ice bath. Afterwards, hydrogen peroxide was slowly added (1.7871 g of solution, 50 wt%, 26.28 mmol) and later, anhydrous citric acid (0.6817 g, 3.55 mmol). HMTD started to precipitate within 2 h, in contrast to the 5 to 6 h required without formaldehyde. The reaction was allowed to continue overnight as the ice bath warmed up. Aliquots of the reaction mix were taken every 0.5 h for 4 h after the addition of the acid, and the final aliquot was taken 27 h later. The crude HMTD was vacuum-filtered, washed with distilled water (ca. 200 mL) to remove acid and HPLC grade methanol (ca. 200 mL) to aid drying (dried several hours by vacuum filtration).

2.4 Synthesis of HMTD with ^{15}N Ammonium Sulfate

HMTD was synthesized from ice-cooled hydrogen peroxide (2.4082 g, 50 wt%, 35.42 mmol) with slow addition of hexamine (0.6061 g, 4.33 mmol) and later addition of anhydrous citric acid (0.9146 g, 4.76 mmol). After the citric acid dissolved, ^{15}N ammonium sulfate was added (0.2874 g, 2.17 mmol). After 4 to 5 h, HMTD began to precipitate from the cold solution. The reaction warmed to room temperature overnight, and crude HMTD was vacuum filtered, washed by gentle agitation with distilled water (ca. 200 mL) to remove acid, then HPLC grade methanol (ca. 200 mL) to aid drying. It was left to dry several hours on the vacuum filter. The crude HMTD yield was about 60% (assuming 1:1 molar ratio hexamine:HMTD).

2.5 Synthesis of ^{15}N Hexamine and HMTD Decomposition Products

Pure ^{15}N hexamine was synthesized by adding formaldehyde (1.7463 g solution, 37 wt%, 21.54 mmol) to ^{15}N ammonium hydroxide (2.3117 g solution, 10.4 wt%, 13.36 mmol) at 40 °C, using a procedure from Nielsen [8]. The reaction mixture was stirred for 2 h, methanol (2 mL) was added, and the water/methanol solution was removed by evaporation at 40 °C. The crude hexamine was purified by sublimation at 185–200 °C; a water aspirator was used to maintain the vacuum. The purified hexamine (397.6 mg, 2.76 mmol) had a melting /sublimation point at 265–275 °C (by Mel-Temp apparatus). GC/MS (gas chromatography with mass spectrometric detection) (144 *m/z*), infrared spectroscopy (IR), and ^{1}H NMR ($CDCl_3$): $\delta = 4.73$, showed good purity. Stirring formaldehyde and formamide at ambient conditions for a day yielded N-(hydroxymethyl)formamide (*m/z* 75, Table 3 entry 3.2) along with hexamine [9]. The synthesis of 1,3,5-triformylhexahydro-s-triazine (*m/z* 171, Table 3 entry 3.11) was accomplished by adding acetic-formic anhydride to hexamethylenetetramine at room temperature, using the method of Gilbert [10]. Tetramethylene diperoxide diamine dialdehyde (TMDDD) was synthesized by the route of Wierzbicki [5]. *N,N′*-methylenebisformamide (*m/z* 102, Table 3 entry 3.5) was purchased from Aldrich.

2.6. Synthesis Conditions of HMTD with a 1-to-1 Mix of ^{14}N and ^{15}N Hexamine

HMTD was synthesized by adding ^{14}N hexamine (304.0 mg, 2.17 mmol) and ^{15}N hexamine (304.0 mg, 2.11 mmol) to hydrogen peroxide (2.4077 g of solution, 50 wt%, 35.41 mmol). Anhydrous citric acid was added (0.9154 g, 4.76 mmol), and the reaction mixture was allowed to stir overnight as the ice bath warmed up. Aliquots were taken every hour until the HMTD precipitated after 6 h. The final aliquot of the reaction mix was taken after 19 h. The crude HMTD was vacuum-filtered, washed with excess distilled water (ca. 200 mL) to remove acid, then HPLC grade methanol (200 mL) to aid drying, and left to dry several hours on the vacuum filter.

2.7 Isothermal Decomposition

HMTD was aged neat and with additives of interest. Typically samples, about 20 mg total, were heated at 60 °C or 80 °C in an oven for varying lengths of time. For testing the compatibility of HMTD with common reagents, liquids (200 μL) were added to some samples and solids (ca. 3.5 mg, i.e. 15 wt%) were added to other samples. Most samples were stored in open vials which were sealed inside larger (10 mL) headspace vials (with humidity controlling solution between inner and outer vial) or held in humidity-controlled desiccators. Other samples were sealed directly in 10 mL headspace vials with no attempt to control humidity. Humidity was controlled with Drierite [considered 0% relative humidity (RH)], saturated $MgCl_2$ (considered 30% RH), saturated NaCl (considered 75% RH), and distilled water (considered 100% RH) [11]. At the completion of the aging cycle, vials were opened under 20–40 mL of acetonitrile. If the HMTD additive was an aqueous solution, magnesium sulfate was added to the sample as a drying agent; if the additive was acidic or basic, sodium hydrogen carbonate was added to neutralize. The acetonitrile solution was sonicated for at least 30 min and vortex mixed for 1 min. If the solutions were cloudy, they were syringe filtered into vials for analysis.

2.8 Decomposition of HMTD with ^{15}N Ammonium Sulfate

^{15}N ammonium sulfate at 15 wt%, was added to HMTD (20 mg), and the mixture was heated at 80 °C under dry conditions or at 60 °C under 75% RH. After thermolysis, samples were extracted with 30 mL of acetonitrile and analyzed by GC/MS and on LC/MS (liquid chromatography with mass spectrometric detection) in order to monitor incorporation of ^{15}N into the condensed-phase decomposition products.

2.9 Decomposition of HMTD with Deuterium Oxide High Humidity

HMTD (20 mg) was heated at 60 °C in a small vial, which was sealed in a 10 mL headspace vial with 1 mL of deuterium oxide (D_2O) between the inner and outer vials so that HMTD did not directly make contact. HMTD was decomposed in a similar configuration with a saturated NaCl/D_2O solution (analogous to 75% RH conditions) between outer and inner vials for 5 d. The pH of the D_2O and analogous experiments with water was found to be highly acidic (pH of 1). These samples were extracted with acetonitrile (30 mL), and run on GC/MS and on LC/MS to track the exchange of deuterium into the condensed phase decomposition products. Headspace analysis was also conducted according to the method described in section 2.13 using SPME. NMR (^1H and ^{13}C) of the D_2O in the vial was used to identify formic acid (HCOOH). ^1H NMR (D_2O): $\delta = 8.13$ (s, 1 H). ^{13}C NMR: $\delta = 167.25$.

2.10 Differential Scanning Calorimeter (DSC)

DSC samples were prepared by measuring 150 to 200 µg of sample into a glass capillary tube, which was then flame sealed. For samples with an additive, 5 to 30 wt% additive was gently stirred into a 20 mg HMTD sample, and this mixture was placed in the capillary tube. If additives were liquid, 2 µL of the liquid was added to 150–200 µg of HMTD, and then sealed in capillary tubes. The sealed micro-ampules were weighed before and after DSC analysis to verify no leakage during testing. Samples were run on a TA Instruments Q100 DSC from 25 to 300 °C with a ramp rate of 20 K min^{-1} in a nitrogen flow. Results were processed via TA's Universal Analysis software.

2.11 Monitoring Rate of HMTD Formation

Aliquots (100 µL) were removed and diluted with 5 mL of HPLC grade acetonitrile with sodium hydrogen carbonate and magnesium sulfate added to neutralize acid and dry the solvent, respectively. This mixture was then diluted 1/10 v/v and analyzed by GC/MS.

2.12 Condensed Phase Analysis – GC/MS

Analysis of the acetonitrile samples, generated as described above, was accomplished using an Agilent 6890 gas chromatograph with a 5973 Mass Selective Detector (GC/MS) equipped with a Varian VF-200ms column (15 m × 0.25 mm). Two different GC/MS methods were used, one for quantification of HMTD and one for qualitative analysis of more volatile compounds. Common to both methods were the following: inlet and transfer line temperatures were maintained at 150 °C, the inlet was kept in splitless mode; flow rate, constant at 2.5 mL min^{-1}, and the post-run oven temperature was always 310 °C for 3 min. The oven temperature program for the quantification method of HMTD started at 120 °C, and was held for 1 min, ramped 20 K min^{-1} to 140 °C and was held for 2 min, and then ramped 10 K min^{-1} to 250 °C. The mass spectrometer scan parameters for the quantification of HMTD were from 50–350 *m/z* at a rate of 4.72 scans per s. The oven temperature program used for qualitative analysis (i.e. product identification) started at 50 °C and was held for 1 min, ramped 20 K min^{-1} to 140 °C and was held for 2 min, then ramped 10 K min^{-1} to 250 °C. The mass scan parameters were from 15–450 *m/z* at a rate of 3.35 scans per s.

2.13 Headspace Analysis – GC/MS

Headspace of the HMTD was sampled via gas-tight syringe (5 µL or 1 mL) or solid phase microextraction (SPME) fiber (SUPELCO fused silica coated with 65 µm of PDMS/DVB). The former was used for permanent gases; the latter for volatile amines. SPME fibers were flushed under helium 45 min at 250 °C prior to use. They were exposed to the samples for at least 3 h at room temperature and analyzed using a Thermo GC Ultra-ISQ GC/MS equipped with a Pora-Plot Amines column (25 m × 0.32 mm) and a 2 m particle trap. Initial oven temperature was 100 °C, with a 20 K min^{-1} heating ramp to 220 °C where it was held 20 min. Inlet temperature was 220 °C; and column was used in constant pressure mode (10 psi). MS scans were from 35–200 *m/z* at 5 scans per s; transfer line and source were at 220 °C. Permanent gases were analyzed with an Agilent 6890 GC with 5973 MS detector with Mol sieves 5A Plot column (10 m × 0.32 mm); initial oven temperature was 70 °C for 1 min, followed by a 50 K min^{-1} ramp to 300 °C and held there for 15 min. Transfer line was set at 300 °C; the flow rate, at 2.5 mL min^{-1}. Two injection methods were used. A 5 µL injection with 5 : 1 split ratio was used to detect O_2 and N_2 signals; a 1 mL injection with a 1 : 1 split ratio was used for traces of other small molecules. The mass spectrometer scan parameters were from 10 to 100 *m/z* at12.89 scans per s.

2.14 Condensed Phase Analysis – LC/MS

Liquid chromatography/mass spectrometry (LC/MS) analysis was conducted using modified procedures recently published [12]. HMTD samples were typically provided as approximately 1 $\mathrm{mg\,mL^{-1}}$ solutions in acetonitrile. Samples were diluted by placing 10 μL of this solution into 1 mL of 50/50 (v/v) acetonitrile/water. Injections of 20 μL (ca. 200 ng) were made onto the HPLC/MS system. Data collection and analysis was performed with Thermo Xcalibur software version 2.2, SP 1.48. Using a Thermo Electron (Franklin, MA, USA) Exactive Orbitrap mass spectrometer affixed with an atmospheric pressure chemical ionization (APCI) interface, positive ions were produced and introduced into the instrument. Tune conditions were as follows: spray voltage 5000 V; capillary temperature 140 °C; sheath gas (N_2) 30; auxiliary gas (N_2) 15; heater temperature 160 °C; capillary voltage 40 V; tube lens 160 V; and skimmer, 15 V. Units for sheath and auxiliary gas flow are arbitrary. Liquid chromatography was performed using a Thermo Electron Accela quaternary pump. Sample injections were performed by a CTC Analytics (Zwingen, Switzerland) HTS PAL autosampler.

Due to the highly polar nature of the decomposition products, three methods were employed to identify these compounds. Initial reverse phase chromatography used a Thermo Scientific (Franklin, MA, USA) Hypersil C-18 (2.1 × 100 mm, 5 μm) column. This method consisted of an initial mobile phase of 95 % solvent B (0.1 % acetic acid) and 5 % solvent C (acetonitrile). It was held for 2 min and then linearly ramped to 5 % B and 95 % C over 18 min. This was held for 2 min, returned to initial conditions over 1 min and the re-equilibrated for 5 min. A second HPLC system was developed for optimum analysis of HMTD and hexamine; it employed an Advantage PFP column (100 × 2.1 mm, 5 μm) (Analytical Sales & Service, Pompton Plains). In order to gain some retention of hexamine, neutral pH conditions were preferable, but this caused broadening of the HMTD peak shape. To remedy this problem, three different mobile phase solvents were used to provide both pH and solvent strength gradients. Initially, 95 % solvent A (10 mM ammonium acetate, pH 6.8) and 5 % solvent C (acetonitrile) were held for 3 min following injection to retain hexamine. The system was rapidly ramped to 85 % solvent B (0.1 % acetic acid), 5 % solvent A, and 10 % solvent C over the next 3 min. Organic levels increased slowly for 9 min to 35 % C, 60 % B and 5 % A, then rapidly for 3 min to 90 % C and 5 % of both A and B. This was held for 2 min before returning to initial conditions and re-equilibrated for 5 min prior to the next injection. Although this method revealed HMTD and most of the decomposition products, e.g. hexamine, a substantial number of species were still so polar that they were negligibly retained by this method. A third system employed an aqueous normal phase method using an Analytical Sales and Service Advantage 100 Silica column (150 mm × 2.1 mm, 5 μm). Initial conditions of 95 % solvent C and 5 % solvent D (methanol) were held for 2 min before ramping to 5 % C and 95 % D over 6 min. Solvent C was replaced with solvent B over 1 min and then ramped to 60 % B to 40 % D over 10 min. After holding this for 2 min, it was ramped back to 95 % D and 5 % B over 2 min, then 95 % D and 5 % C over 1 min. Initial conditions were returned over 2 min and held for 5 min before the next injection. This method required the use of electrospray ionization (ESI); however, this ionization mechanism is not optimal for HMTD detection.

3 Results and Discussion

Previously reported were thermal decomposition kinetics of HMTD determined by manometry (E_a 107 $\mathrm{kJ\,mol^{-1}}$ and $A = 4.21 \times 10^{10}\ \mathrm{s^{-1}}$) and HMTD fragmentation by electron impact mass spectrometry [13–15]. Herein, we examine factors, which influence the stability of HMTD. It is the standard protocol of this lab that following synthesis a purification step is performed to promote stability. Unfortunately, HMTD had only limited solubility even in the most polar solvent requiring large volumes of ethyl acetate and acetonitrile for recrystallization, which were almost impossible to remove completely from HMTD. For that reason, many of the studies were conducted with both crude and recrystallized HMTD to ensure the presence of trace solvent had not biased results.

3.1 HMTD Headspace

Since HMTD decomposition was readily observed at 60 °C, significant decomposition at ambient temperature was probable. In fact, when HMTD was removed from storage at −15 °C (freezer temperature), it developed a noticeable odor after a couple of hours. Headspace samples of both crude and recrystallized HMTD, fresh and aged, were analyzed by GC/MS. When HMTD was heated for a week at 60 °C in 30 % relative humidity, or under a variety of conditions, the predominant decomposition products observed in the headspace were trimethylamine (TMA) and dimethylformamide (DMF) with trace quantities of ethylenimine (EN), methyl formamide (MFM), formamide (FM), and hexamine. When moisture was present 1-methyl-1H-1,2,4-triazole and pyrazine were observed. Figure 1 shows that these compounds were found in headspace of HMTD sample stored at room temperature for one year. In addition, while permanent gases, oxygen and nitrogen, were not found, carbon monoxide and carbon dioxide occurred in significant amounts. HMTD was not observed in the headspace by GC/MS under dry, moist, acidic, or basic conditions. Since HMTD could be identified in ACN solutions, either HMTD content in headspace was below the detection limits of our GC/MS system or due to its reactivity, occurrence was not sustainable in the headspace.

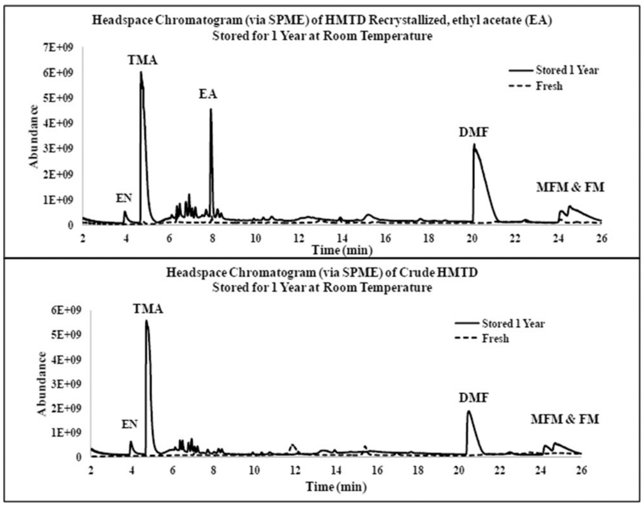

Figure 1. HMTD headspace chromatography [trimethylamine (TMA), dimethylformamide (DMF), ethylenimine (EN), methyl formamide (MFM), formamide (FM)].

3.2 Effect of Additives on HMTD Decomposition

The effect of additives on HMTD stability was screened by DSC. A general trend was readily observed: acids lower the temperature at which the exothermic maximum appeared (Table 1). We had previously demonstrated that concentrated mineral acid could be used to destroy HMTD [16]. We and others also observed that aqueous basic solutions rapidly decompose HMTD [17]. To determine the effect of select additives without water, HMTD was held at 60 °C for a week at 30 % RH, and of these additives, only citric acid markedly accelerated HMTD decomposition (Table 2). The fact that water and citric acid, both used in the synthesis of HMTD, lowered its thermal stability markedly emphasizes the need to thoroughly rinse and dry HMTD. Headspace monitoring revealed that water, citric acid or any acidity sped up the production of TMA and DMF in the gas phase.

3.3 Effect of Humidity on HMTD Decomposition

In 1924, it was reported "that H. M. T. D. is stable at temperatures up to at least 60 °C; it is not affected by storage under water; but it is slowly affected when subjected to high humidity at maximum summer temperature… It is practically non-hygroscopic" [17]. Since DSC results did not support this statement, samples of crude HMTD were held at 60 °C with fixed humidity values of 0, 30, 75, or 100 % RH and monitored each week for four weeks (Figure 2). After two weeks, the samples of HMTD at high relative humidity (i.e. 75 % RH and 100 % RH) were completely degraded; HMTD was not observed by GC/MS.

Table 1. Effect of solid additives on HMTD stability.

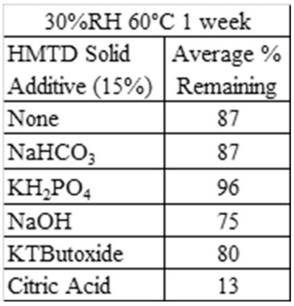

30%RH 60°C 1 week	
HMTD Solid Additive (15%)	Average % Remaining
None	87
$NaHCO_3$	87
KH_2PO_4	96
NaOH	75
KTButoxide	80
Citric Acid	13

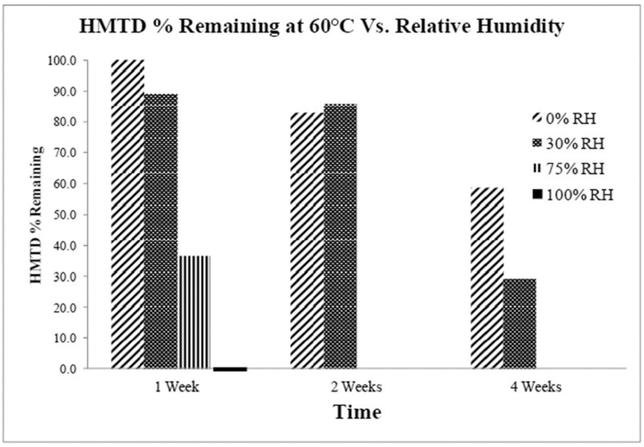

Figure 2. Effect of humidity on HMTD.

In Figure 3 the effects of humidity on crude and recrystallized HMTD are particularly informative. Crude and re-

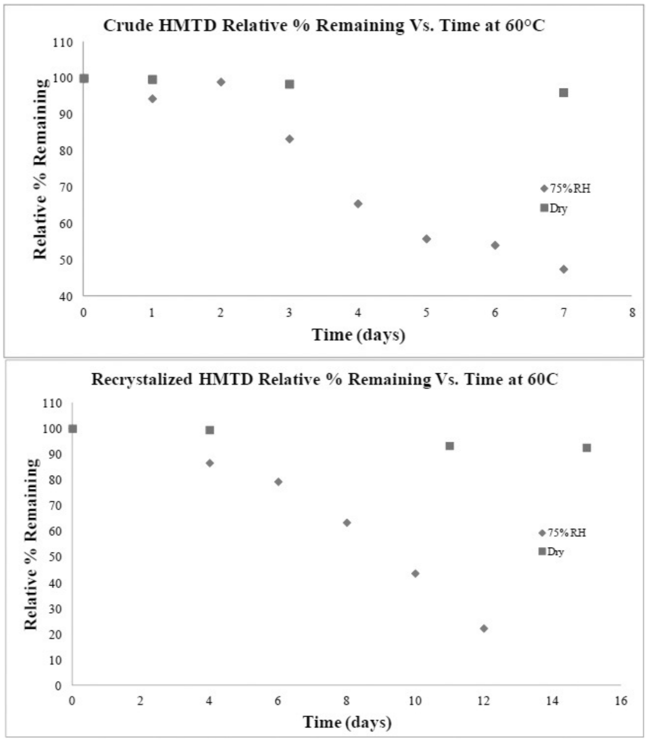

Figure 3. Effect of humidity on crude and recrystallized HMTD.

Table 2. DSC of HMTD with additives (20 K min^{-1}).

Material	pK$_a$ of Additive	pK$_b$ of Additive	Onset Temp. of Exotherm (°C)	Exotherm Temp. Maximum (°C)	Heat Released (J/g)
18.2MΩ H_2O	14.0	0.0			
HMTD Crude	N/A	N/A	159	161	2100
HMTD Rec 70/30 EA/ACN	N/A	N/A	168	171	3200
HMTD + Aqueous Solution					
HMTD Crude + 2ul H_2O	N/A	N/A	136	140	3100
HMTD Rec 70/30 EA/ACN + 2ul H_2O	N/A	N/A	140	143	3200
HMTD Crude + 2ul pH4 Buffer	N/A	N/A	126	129	3700
HMTD Crude + 2ul pH7 Buffer	N/A	N/A	134	137	3300
HMTD Crude + 2ul pH10 Buffer	N/A	N/A	137	139	3100
HMTD + Solvents					
HMTD Crude + 2ul ACN	N/A	N/A	152	178	3000
HMTD Crude + 2ul Benzene	N/A	N/A	166	172	3200
HMTD Crude + 2ul EtOH	N/A	N/A	153	164	2800
HMTD Crude + 2ul EtAc	N/A	N/A	156	169	2800
HMTD + Solid Acids					
HMTD Crude + KH_2PO_4 15%	7.2	6.8	163	165	2100
HMTD Crude + KH Phthalate 15%	5.4	8.6	156	157	1900
HMTD Crude + Benzoic Acid 15%	4.2	9.8	155	160	2600
HMTD Crude + Ascorbic Acid 15%	4.0	10.0	146	148	2000
HMTD Crude + Citric Acid 15%	3.1	10.9	134	137	2800
HMTD Crude + Sulfanilic Acid 15%	3.0	11.0	122	125	2400
HMTD Crude + O Phthalic Acid 15%	2.9	11.1	143	145	2000
HMTD + Solid Bases					
HMTD Crude + Melamine 15%	5.0	9.0	158	159	2000
HMTD Crude + $NaHCO_3$ 15%	6.4	7.7	163	164	1300
HMTD Crude + KH_2PO_4 15%	7.2	6.8	163	165	2100
HMTD Crude + NaOH 15%	14.0	0.0	160	161	2300
HMTD Crude + NaOH 30%	14.0	0.0	162	164	2100
HMTD Crude + K Tertbutoxide 15%	17.0	-3.0	159	160	2200

*$NaHCO_3$ has an endotherm which lowers the total heat released

crystallized HMTD stored dry at 60 °C undergo only slight decomposition while samples stored at high humidity (i.e. 75 % RH) experience significant decomposition.

3.4 Mass Spectral Analysis of Condensed-Phase Synthesis and Decomposition Products

HMTD was heated at 60 °C under various conditions. Products were examined by GC/MS and LC/MS; and assignments are shown in Table 3 and Table 4, respectively. Assignments are based on comparison with the authentic samples [entry 3.2, 3.5, 3.8, 3.11, 4.2, 4.8, 4.15, 4.22, and HMTD] and on the high resolution mass spectrometric results, where compositions could be assigned to within 5 ppm of their calculated mass (Table 4). Examining the HMTD decomposition products, it is tempting to suggest HMTD thermolysis produces a number of small molecular fragments, e.g. CH_2O, NH_3, CH_2NH, or $CH(O)NH_2$, which undergo further reaction, such as an aldehyde-amine condensation. The observed substituted triazine species (entry 3.10, 3.11, 3.12) and those containing four nitrogen atoms have been reported to be products of hexamethylenetetramine (hexamine) reactions [8, 10, 18]. Indeed, hexamine was found when HMTD was decomposed at 60 °C with 75 % or 100 % RH or with added water or acidic buffer. Only tetramethylene diperoxide diamine dialdehyde (TMDDD) (4.22), matched to an authentic sample and the mono-aldehyde (3.7) suggested the original HMTD structure; and that HMTD was degraded stepwise.

In examining HMTD decomposition, we speculated the degradation products formed hexamine. Hexamine is made from ammonia and formaldehyde, and the route is via hexahydro-1,3,5-triazine [8, 19]. The conversion of hexamine to 2,4,6-cyclotrimethylene-1,3,5-trinitramine (RDX) has been the subject of several studies. Thermal degradation of hexamine forms hexahydro-1,3,5-triazine, octahydro-1,3,5,7-tetrazocine, and 1,3,5,7-tetrazabicyclo-[3.3.1]-nonane [20]. Bachman found that performing the nitration of hexamine in acetic anhydride with ammonium nitrate allowed two moles of RDX to be produced rather than one via direct nitration [21]. The question was whether the extra RDX came from fragments of hexamine or nitramines CH_2NNO_2 or directly from hexamine. On the basis of the observed byproducts, Aristoff et al. concluded that degradation of hexamine, itself, and not combination of smaller fragments, was the route by which RDX is formed [22]. Gilbert also confirmed this later by showing that RDX can be obtained by the direct nitrolysis of substituted triazine rings [10].

In the synthesis of HMTD from hexamine the question of stoichiometry arises. Under the normal synthetic route as it is describe in Equation (1); our yield, based on hexamine, was not more than 60 %. However, if excess formaldehyde was added to the reaction mixture, yields of greater than 100 % (based on one HMTD to one hexamine) were observed, and the reaction rate increases (precipitation of HMTD started to occur in 2 h compared to 5–6 h without formaldehyde). Equation (2) describes that reaction and may also describe what occurs when no extra formaldehyde is added and the reaction must wait for the degradation of part of the hexamine to form formaldehyde (Figure 4). Indeed, hexamine is frequently used as a source of formaldehyde [18, 23].

$$C_6N_4H_{12} + 3H_2O_2 \rightarrow C_6N_2H_{12}O_6 + 2NH_3 \tag{1}$$

$$C_6N_4H_{12} + 6H_2O_2 + 6CH_2O \rightarrow 2C_6N_2H_{12}O_6 + 6H_2O \tag{2}$$

Although not shown in the above reactions, without citric acid formation of HMTD takes days. Furthermore, the reaction is sensitive to the type and amount of acid (Table 5). Diprotic (sulfuric and oxalic) and triprotic (phosphoric) acids could be used as direct replacements for citric acid. Monoprotic acids (acetic acid, trifluoroacetic acid, formic acid, and nitric acid) gave yields comparable to citric acid only if these acids were added in 2.2 mol acid to 1 mol hexamine ratio. This aspect of the acid effect merits further examination.

If HMTD is formed when hexamine breaks into smaller fragments, then it should incorporate carbon and nitrogen from outside sources. When HMTD synthesis was performed with ^{13}C formaldehyde solution, the label appeared in both the HMTD (*m/z* 209, 210, 211, 212, 213) and the hexamine (*m/z* 140, 141, 142, 143, 144) early in the reaction (42 min when precipitation was observed in 2 h). A possible explanation is formation of bis(hydroxymethyl) peroxide (BHMP) and its incorporation into HMTD (Figure 5). Incorporation of formaldehyde into the hexamine can be explained by looking at the first two steps of decomposition of hexamine (Figure 4). Excess formaldehyde may push this reaction in the reverse direction. However, HMTD synthesized in the presence of ^{15}N-labeled ammonium sulfate, showed little incorporation based on GC/MS and LC/MS results.

In contrast to the lack of ^{15}N incorporation during HMTD synthesis, it was found that under humid decomposition conditions, the ^{15}N label was observed in the decomposition products (entries 4.2, 4.12, 4.13, 4.14, 4.15, 4.17, 4.20) as well as in hexamine (single, double, triple, and quadruple label). Yet, when the same decomposition conditions were

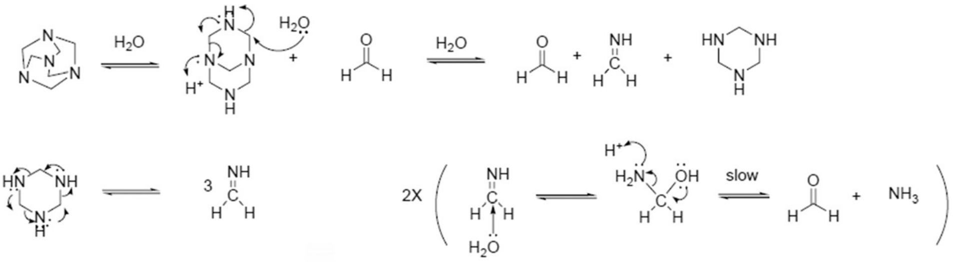

Figure 4. Proposed hexamine decomposition.

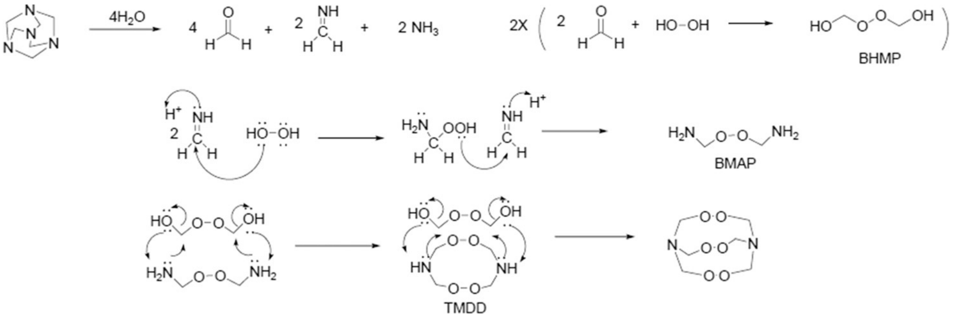

Figure 5. Formation of HMTD from completely dissociated hexamine.

Table 3. Decomposition products GC/MS.

#	m/z	Identity	amount	conditions
3,1	73	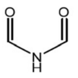	L	DRY (0 %RH) & HUMID (≥75 %RH)
3,2	75	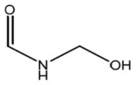	L	MATCHED TO AUTHENTIC SAMPLE; MAINLY SEEN IN HUMID CONDITIONS
3,3	103	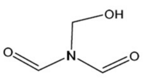	M	MAINLY SEEN IN HUMID CONDITIONS
3,4	88	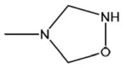	S	
3,5	84, 102	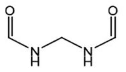	L	MATCHED TO AUTHENTIC SAMPLE; DRY CONDITIONS
3,6	116	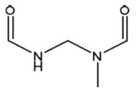	L	DRY CONDITIONS
3,7	178	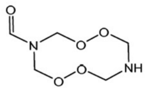	S	BOTH IN DRY & HUMID CONDITIONS
3,8	140	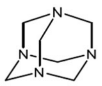	M	MATCHED TO AUTHENTIC SAMPLE; MAINLY SEEN IN HUMID OR ACIDIC CONDITIONS
3,9	208	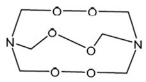	L	
3,10	143	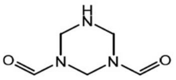	S	
3,11	171	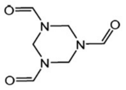	L	MATCHED TO AUTHENTIC SAMPLE; MAINLY SEEN IN HUMID CONDITIONS
3,12	157	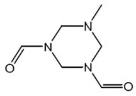	S	MAINLY SEEN IN DRY CONDITIONS

performed dry, no hexamine was formed and the decomposition products 4.2 and 4.14 showed no label incorporation.

In deuterium oxide, HMTD decomposition products trimethylamine, dimethylformamide, hexamine, and triazines showed little incorporation of deuterium (*m/z* 157, 171 etc.). This suggested that hydrogen transferred during the decomposition was from the original HMTD molecule.

A mechanism for HMTD formation was proposed on data from isotopic ratio mass spectrometry [24]. Because it required the formation of a triperoxy tertiary amine and protonated methylene imine, we sought alternative proposals. Tentative proposals are illustrated in Figure 5 and Figure 6. In Figure 5 hexamine is broken into small molecules, and from the formaldehyde/hydrogen peroxide reaction bis(hydroxymethyl) peroxide (BHMP) is formed, while from the imine/ hydrogen peroxide reaction bis(methylamine) peroxide (BMAP) is formed. The latter reacts with 2 molecules of BHMP, forming tetramethylene diperoxide diamine (TMDD) as an intermediate, to create HMTD. The mechanism in Figure 6 also postulates the formation of BHMP but allows hexamine to remain moderately intact until fairly late in the reaction. Both mechanisms speculate that the reaction proceeds to HMTD faster in the presence of excess formaldehyde because formation does not require initial degradation of hexamine into formaldehyde. The key to both mechanisms is the formation of BHMP, first synthesized in 1914 by Fenton from hydrogen peroxide and formaldehyde and later studied by Satterfield [25]. It is likely this species was generated in situ in the reported syntheses of several caged peroxides having planar bridgehead nitrogen atoms [26]. Once a methylene is lost from hexamine as formaldehyde the resulting octahydro-1,3,5,7-tetrazocine would be subject to rapid ring inversion and isomerization from which BHMP could bridge across two nitrogen atoms.

To discriminate between the mechanisms proposed in Figure 5 and Figure 6, synthesis of HMTD was done with a 1 to 1 mixture of ^{14}N hexamine and ^{15}N hexamine. If the formation of HMTD proceed through the route shown in Figure 5, then complete scrambling of the label would be expected, i.e. the HMTD product should show the unlabeled, single-labeled and double-labeled species [M+H], 209 to 210 to 211, in a 1 to 2 to 1 ratio. Indeed that was what was observed (Figure 7).

To shed light on the question of how HMTD decomposes, density functional theory (DFT) calculations were performed. The initial sequence of steps in the decomposition of a single HMTD molecule is described in Figure 8. Energy differences of the transition states and entropies of the various species along the decomposition pathway were calculated relative to the energy of the nearest intermediate or reactant to show energy barrier and entropy change for each decomposition reaction step. The calculations were carried out for both gas phase molecule (values without parenthesis) as well as for a solvated molecule in water (values in parenthesis). The structure and properties of the various intermediate species along the decomposition pathway are summarized in Table 6.

(1) First step via TS1 consists of O–O bond opening together with hydrogen atom transfer from the methylene group (CH_2) near one of the oxygen atom to the oxygen atom farther away. The transition state is an open shell singlet state (bi-radical). This is the rate-limiting step in the decomposition process. Following TS hydrogen transfer, O–O

Table 4. Decomposition products LC/MS.

#	[M+H]$^+$	Identity	amount	empirical formula [M+H]$^+$
4,1	74,06004	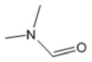	L	C3H8ON
4,2	103,0501	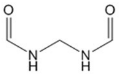	L	C3H7O2N2 MATCHED TO AUTHENTIC SAMPLE
4,3	106,0499	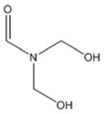	S	C3H8O3N
4,4	117,0659	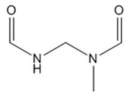	L	C4H9O2N2
4,5	117,1022	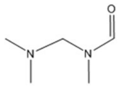	L	C5H13ON2
4,6	120,0768	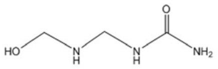	S	C3H10O2N3
4,7	133,0608	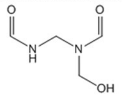	S	C4H9O3N2
4,8	141,1131	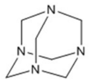	L	C6H13N4 MATCHED TO AUTHENTIC SAMPLE
4,9	144,0768	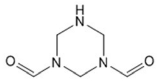	M	C5H10O2N3
4.10	145,0608	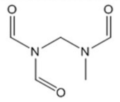	M	C5H9O3N2
4,11	155,1289	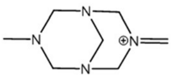	M	C7H15N4
4,12	157,1083	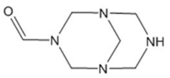	L	C6H13ON4
4,13	158,0923	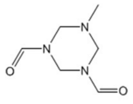	L	C6H12O2N3
4,14	160,0717	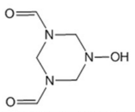	L	C5H10O3N3
4,15	172,0712	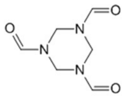	L	C6H10O3N3 MATCHED TO AUTHENTIC SAMPLE
4,16	172,1078	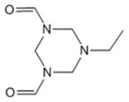	S	C7H14O2N3
4,17	174,0873	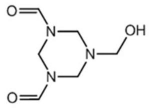	M	C6H12O3N3
4,18	174,1235	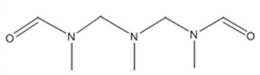	S	C7H16O2N3
4,19	185,1032	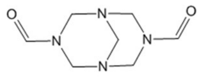	S	C7H13O2N4
4.20	201,0982	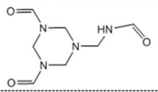	L	C7H13O3N4
4.21	205,0931	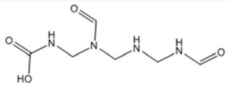	S	C6H13O4N4
4.22	207,0611	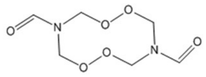 TMDDD	M	C6H11O6N2 MATCHED TO AUTHENTIC SAMPLE
4.23	209,0768	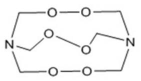 HMTD	M	C6H13O6N2

Table 5. HMTD reactions with additives with scaled yield of 0.5 g.

HMTD Reaction #	Additive	Mol Ratio of HP (48.4wt%): Hexamine	Mol Ratio Acid (Citric): Hexamine	% Yield	MP (°C)	Purity by GC/MS
5	citric acid	8	1.1:1	44.5	149-150	87.4
6	citric acid	8	1.1:1	40.7	144-145	87.1
17	citric acid	8	1.1:1	52.7	153-157	95.8
14	anhydrous oxalic acid	8	1.1:1	45.0	151-153	94.4
15	85% o-phosphoric acid	8	1.1:1	26.9	149-150	91.3
32	50% sulfuric Acid	8	1.1:1	50.5	152-158	98.2
13	glacial acetic acid	8	1.1:1	7.4	152-153	94.3
30	glacial acetic acid	8	2.2:1	33.1	151-156	100.0
21	88% formic Acid	8	1.1:1	6.3	154-158	94.5
25	88% formic Acid	8	2.2:1	43.5	153-154	100.0
22	99% TFA	8	1.1:1	3.3	155-159	93.3
26	99% TFA	8	2.2:1	53.5	153-156	99.6
31	70% nitric Acid	8	2.2:1	51.1	155-157	100.0
Kin. #2	no acid	8	0:1	9.5	148-149	89.5
Kin. #3	no acid	8	0:1	7.2	152-160	92.4

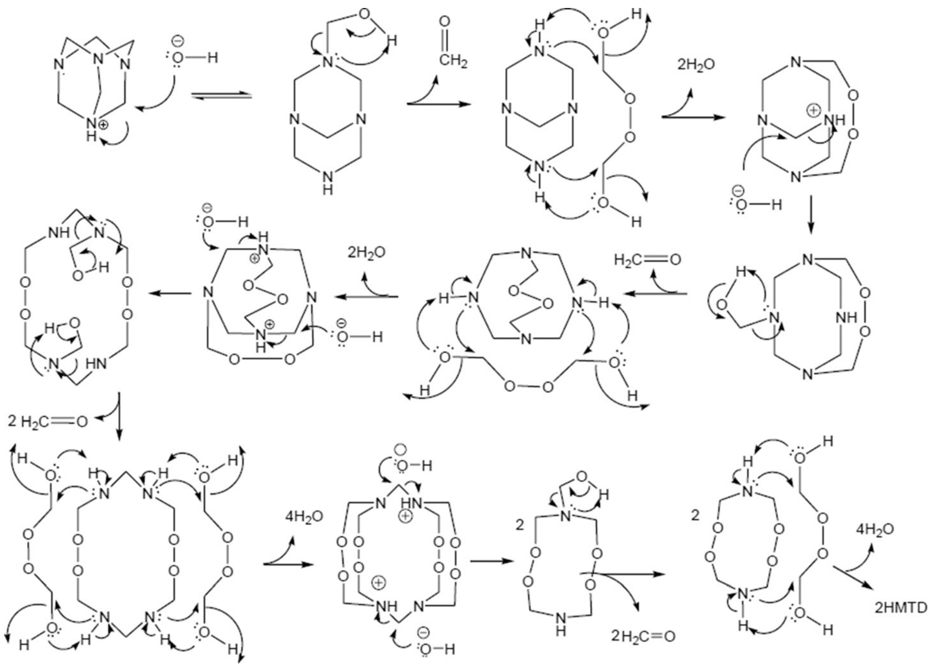

Figure 6. Formation of HMTD from intact of hexamine.

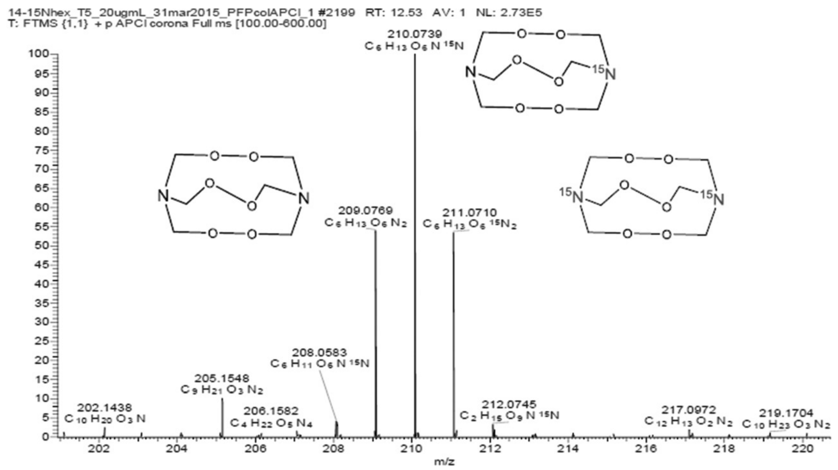

Figure 7. Mass spectrum of HMTD formed from a mixture of N-14 and N-15 labeled hexamine.

bond ruptured results in formation of –OH and –C=O groups, respectively, in INT1.

(2) Second step via TS2 is similar to the first step (1) and leads to rupture of second O–O bond and a second hydrogen transfer to form two new –OH and –C=O groups in INT2.

(3) Third step via TS3 involves an N–C bond opening concerted with hydrogen atom transfer from oxygen atom in CH_2OH group to oxygen atom in –CH=O group to yield INT3 and a formaldehyde molecule.

The following step in this pathway is the decomposition of INT3 into two new species or isomerization into a 7-member ring as shown in Figure 9. The formation of two radials, INT4 and INT5, is favorable according to the entropy changes; however, INT6 formation should be favorable due to a lower energy barrier to overcome.

Next, we considered the decomposition of the HMTD molecule in an acidic environment. A proton can attach to either an oxygen atom or a nitrogen atom. Protonated HMTD forms spontaneously without an appreciable energy barrier. When a proton is attached to one of the nitrogen atoms, the first step in decomposition of the cation will proceed via a C–N bond rupture. The energy barrier associated with this event is much higher than that obtained for the first step in the decomposition of a protonated oxygen atom in the HMTD molecule. Moreover, the barrier associat-

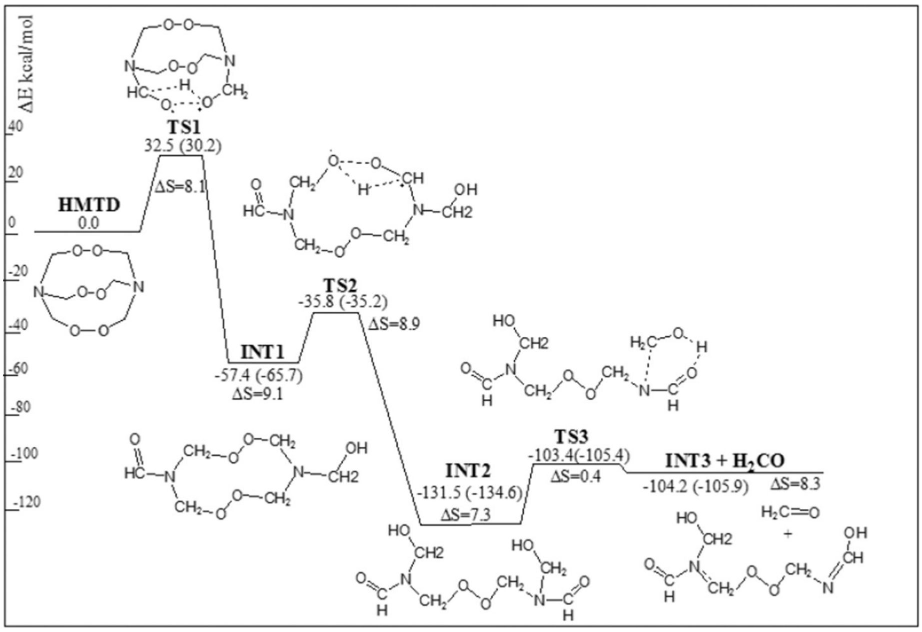

Figure 8. Decomposition route of an isolated HMTD molecule. Energy barriers and energies of intermediates for a gas phase molecule are without parenthesis while values of solvated molecule (in water) are in parenthesis.

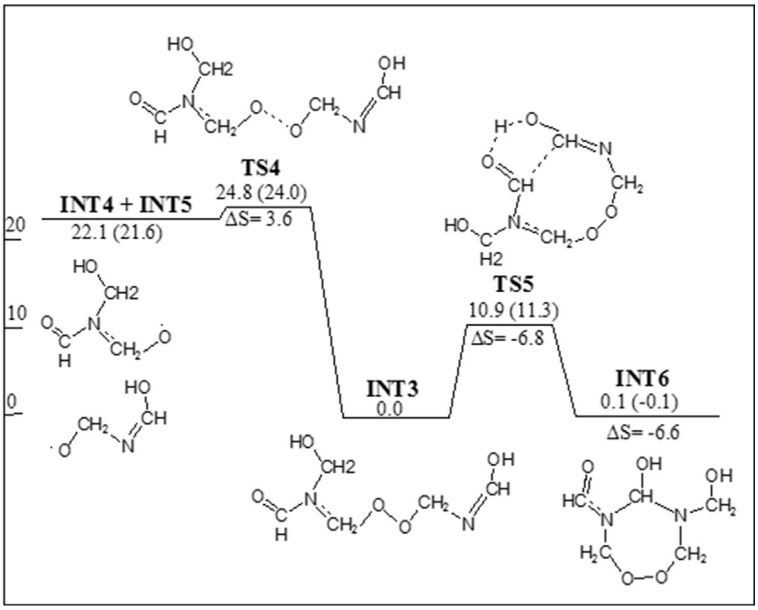

Figure 9. The next steps in the decomposition of an isolated HMTD molecule. Energy barriers and energies of intermediates for a gas phase molecule are without parenthesis while values of solvated molecule (in water) are in parenthesis.

ed with the oxygen atom protonation is also smaller than the magnitude of the energy barrier associated with TS1 in Figure 8. A summary of the energy barriers related to the possible initial steps in the different decomposition schemes are shown in Figure 10. In the case of oxygen atom protonation we revealed two possible decomposition routes that are denoted as path A and path B. The intermediates for these two paths are named INTHOA and INTHOB, respectively. The main difference between these two decomposition routes is that path A proceeds via C–O bond opening, whereas path B occurs via O–O opening. A summary of the structures and properties of all the intermediate species along path A and path B are described in Table 7 and Table 8, respectively.

Table 6. Structure and properties of intermediate species observed during the decomposition of a gas phase HMTD molecule. The calculations were performed using PBE0PBE1/cc-pVDZ level of theory. Energy values in kcal mol^{-1}, entropy values in cal K^{-1} mol^{-1}.

#	mass	structure		name	Kinetic & thermochemical	Reaction step producing intermediate
1	208	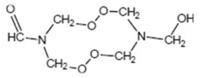	C6H12O6N2	INT1	$\Delta E^{\#}$ =32.5 (30.2), $\Delta S^{\#}$ =8.1 ΔE_{react} = -57.4 (-65.7), ΔS_{react} = 9.1 One O-O bond opening together with H-atom shift from methylene group to oxygen	HMTD → INT1
2	208	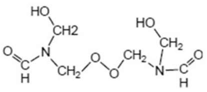	C6H12O6N2	INT2	$\Delta E^{\#}$ =27.3(26.8), $\Delta S^{\#}$ =8.9 ΔE_{react} = - 68.3 (-69.0), ΔS_{react} = 7.3 relative INT1 ΔE_{react} = - 131.5 (-134.6), ΔS_{react} = 16.4 relative HMTD Second O-O bond opening together with H-atom shift from methylene group to oxygen	INT1 → INT2
3	178	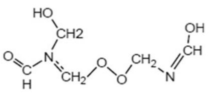	C5H10O5N2		ΔE_{react} = 27.2 (28.7), ΔS_{react} = 8.7 relative INT2 ΔE_{react} = - 104.2 (-105.9), ΔS_{react} = 25.0 relative HMTD	INT2→ → INT3+ H_2CO
4	104	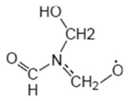	C3H6O3N (radical)	INT4	INT4 + INT5 $\Delta E^{\#}$ =24.8 (24.0), $\Delta S^{\#}$ =3.6 ΔE_{react} = 22.1 (21.6), ΔS_{react} = 10.9 relative INT3	INT3 → INT4 + INT5
5	74	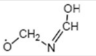	C2H4O2N (radical)	INT5		
6	178	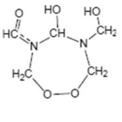	C5H11O5N2	INT6	$\Delta E^{\#}$ =10.9 (11.3), $\Delta S^{\#}$ = -6.8 ΔE_{react} = 0.1 (-0.1), ΔS_{react} = -6.6 relative INT3	INT3 → INT6

As stated above, protonated HMTD is formed spontaneously without any appreciable energy barrier. The rupture of a C–O bond occurs with a minor energy barrier of approx. 3.5 kcal mol^{-1} (path A). The formation of INT2HOA requires overcoming a slightly larger energy barrier; but this barrier is much smaller than that required for HMTD decomposition as a gas phase molecule, TS1. Additional steps in the decomposition of INT2HOA require surmounting a barrier of about 35 kcal mol^{-1}. However the presences of anions in the solution suggest another possible pathway. The third intermediate, INT3HOA is formed following the stabilization of INT2HOA by an anion (OH^- in this case). This neutralization is accompanied by a large energy release. If the OH^- is replaced by H_2O, only a very low barrier is observed. The decomposition of INT3HOA requires overcoming a barrier of about 24 kcal mol^{-1} (see Table 7) and it leads to the formation of two 5-member ring radicals.

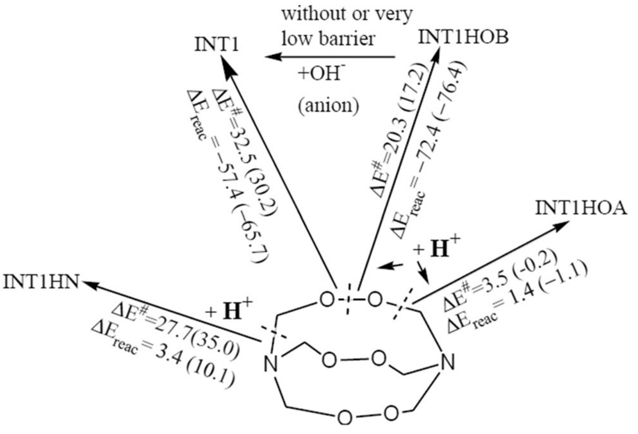

Figure 10. Scheme showing all the possible initial decomposition steps of HMTD molecule in different environments.

The structure and characteristics of the intermediate species in path B of HMTD with protonated oxygen are presented in Table 8. The most important in this route is the possibility that INT1HOB is neutralized by an anion (several anions were tested, OH^-, Cl^-, SO_4^{2-}, HSO_4^-) to produce INT1 shown for neutral decomposition in Figure 8 and as entry 2 in Table 8. This pathway allows one to return to the neutral HMTD decomposition without the necessity to overcome a barrier 32.5 (30.5) kcal mol^{-1}.

Most neutral intermediates can be protonated without an appreciable energy barrier. The intermediates described in Table 8 suggest the possible intermediates with quite large molar mass similar to those presented in Table 3 and Table 4. All these decomposition steps proceed without barriers or with small energy barriers; hence, most of these species are accessible. The highest barrier is related to the formation of formaldehyde (entry 6, Table 8). We also tested the fate of the relatively stable intermediate INT2 (entry 2, Table 6). The structure and properties of the intermediates observed during the decomposition of its protonated form are presented in Table 9.

All the decomposition steps that lead to the formation of these intermediates proceed via barriers smaller than 3 kcal mol^{-1}. In most cases a much lower barrier or even no barrier is associated with the intermediate. Most of the species listed in Table 9 are rather small and resemble some of the species listed in Table 3 and Table 4. Protonation of a nitrogen in the HMTD molecule as the initial step was also considered. The attachment of a proton to nitrogen is preferred by 2.2 kcal mol^{-1} over its addition to one of the oxygen atoms in the molecule; however, there are only two nitrogen atoms compared to six oxygen atoms in an HMTD molecule. The initial steps in the decomposition of a nitrogen protonated HMTD are shown in Figure 11.

Table 7. Structure and properties of intermediate species observed along path A during the decomposition of HMTD molecule with a protonated oxygen. The calculations were performed using PBE0PBE1/cc-pVDZ level of theory. Energy values in kcal mol^{-1}, entropy values in cal K^{-1} mol^{-1}.

#	mass	structure		name	Kinetic and thermochemical characteristics	Reaction step and comments
1	209	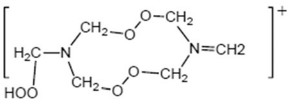	C6H13O6N2	INT1HOA	$\Delta E^{\#}$ =3.5 (-0.2), $\Delta S^{\#}$ =3.6 ΔE_{react} = 1.4 (--1.1), ΔS_{react} = 5.9 C-O bond openning	HMTD (protonated) → INT1HOA Back reaction is possible with large probability
2	209	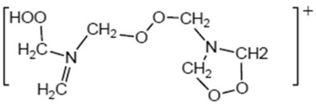	C6H13O6N2	INT2HOA	$\Delta E^{\#}$ =10.0 (14.3), $\Delta S^{\#}$ = 6.6 ΔE_{react} = 5.9 (6.9), ΔS_{react} = 16.5 relative HMTD protonated	INT1HOA → INT2HOA
3	208	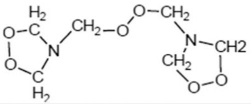	C6H12O6N2	INT3HOA	Without barrier	INT2HOA + OH^- → INT3HOA +H_2O
4	104	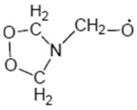	C3H6O3N	INT4HOA	$\Delta E^{\#}$ =24.6 (22.6), $\Delta S^{\#}$ = 9.1 ΔE_{react} = 31.9 (26.2), ΔS_{react} = 47.5 relative INT3HOA	INT3HOA → IN43HOA + INT4HOA

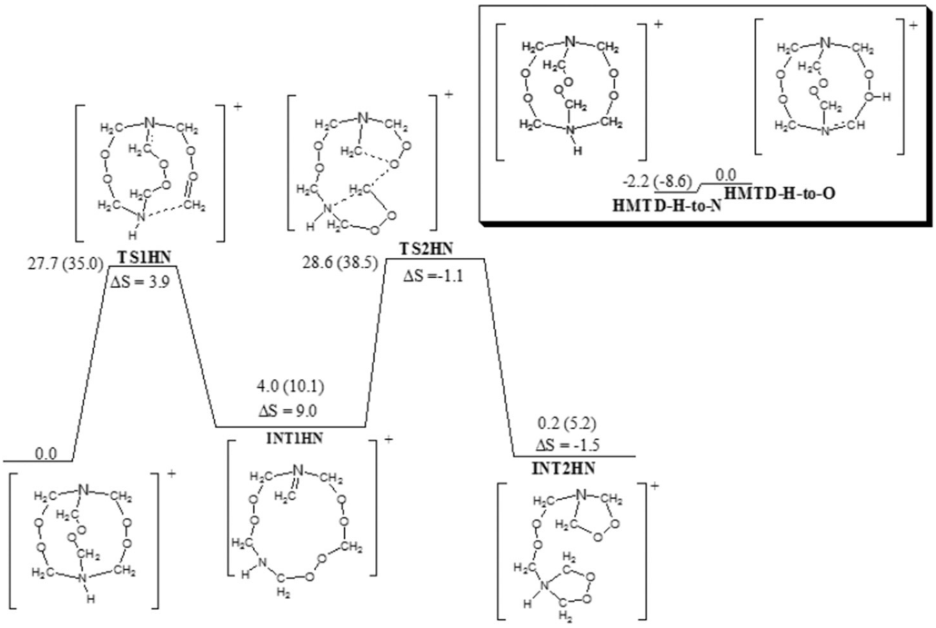

Figure 11. Initial decomposition steps of a nitrogen protonated HMTD molecule.

Table 8. Structure and properties of intermediate species observed along path B during the decomposition of HMTD molecule with a protonated oxygen. The calculations were performed using PBE0PBE1/cc-pVDZ level of theory. Energy values in kcal mol^{-1}, entropy values in cal K^{-1} mol^{-1}.

#	mass	structure		name	Kinetic & thermochemical	Reaction step & comments
1	209	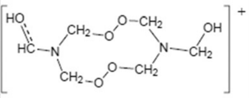	C6H13O6N2	INT1HOB	$\Delta E^{\#}$ =20.3 (17.2), $\Delta S^{\#}$ =8.1 ΔE_{react} = -72.4 (--76.4), ΔS_{react} = 7.9 One O-O bond openning	HMTD (protonated) → INT1HOB
2	208	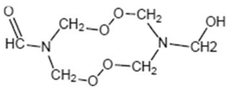	C6H12O6N2	INT1	Without barrier if reagent is OH^- If reagent is H2O $\Delta E^{\#}$ =2.2 (0.9), $\Delta S^{\#}$ = -6.5 ΔE_{react} = 1.0 (-1.4), ΔS_{react} = -3.9 relative INT1 + H_2O	INT1HOB + OH^- → INT1 + H_2O Or INT1HOB + H_2O → INT1 + H_3O^+
3	207	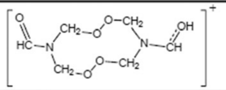	C6H11O6N2	INT2HOB	Without barrier	INT1 + H^+ → INT2HOB + H_2 H+ attack to carbon in terminated CH_2OH group
4	209	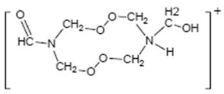	C6H13O6N2	INT3HOB	Without barrier ΔE = -2.8 (-8.6), ΔS = -28.8 relative INT2HOB + H_2	INT1 + H^+ → INT3HOB H+ attack to nitrogen connected with terminated CH_2OH group
5	206	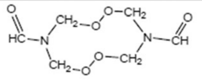	C6H10O6N2	INT4HOB	Without barrier	INT2HOB + OH^- → INT4HOB + H_2O
6	179	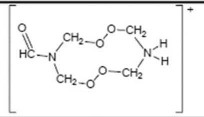	C5H11O5N2	INT5HOB	$\Delta E^{\#}$ =22.1 (29.5), $\Delta S^{\#}$ = 2.5 ΔE_{react} = 11.5 (7.4), ΔS_{react} = 44.5 relative INT3HOB	INT3HOB → INT5HOB + H_2CO
	178	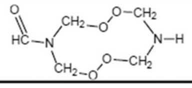	C5H10O5N2	INT8HOB	Without barrier	INT5HOB + OH^- → INT6HOB + H_2O

The first transition state, TS1HN, requires the system to overcome an energy barrier of about 28 kcal mol^{-1} or about 20% lower than that required to reach TS1 in gas phase HMTD decomposition. In TS1HN one C–N and one C–O bonds start to break together with a rearrangement of the molecular structure. Surmounting this energy barrier leads to the formation of a ring shape intermediate that contains three peroxide bonds. A second energy barrier, with similar magnitude to the first one, leads to TS2HN and is followed by ring opening to form INT2HN. This intermediate has two five member rings attached to each nitrogen atom, each ring connected by a –O–O–CH_2–O–O– chain. Further decomposition of INT2HN was examined but did not lead to the formation of stable end products.

We also examined the possible decomposition of HMTD in a basic solution. A sequence of a few steps with relatively low energy barriers separating them (highest is 17 kcal mol^{-1}) and formation of an intermediate with large (104 kcal mol^{-1}) energy release occurs. During this sequence a few formaldehyde molecules were released together with the formation of different intermediate species. The structure and the properties of the different intermediate species along the decomposition pathway are described in Table 10. Thus, HMTD decomposition is also expected to occur in basic environment as was observed in the Experimental Section of this study.

4 Conclusions

Since HMTD is destabilized by water and citric acid, it is important to purify it after initial synthesis. It is recommended to rinse with water to remove acid, then with methanol to remove water. Ignoring the degrading effects of water and acid may lead to an unexpected violent reaction during storage and handling. Precautions for storage should be taken to see that HMTD remains dry and cold. Work to elucidate mechanisms of HMTD decomposition continues, but it appears that the headspace of HMTD is mainly trimethylamine (TMA) and dimethylformamide (DMF); these might

Table 9. Structure and properties of intermediate species observed during the decomposition of gas phase HMTD molecule starting with a protonated INT2 (see Figure 8). The calculations were performed using PBE0PBE1/cc-pVDZ level of theory. Energy values in kcal mol^{-1}, entropy values in cal K^{-1} mol^{-1}.

#	m/e	Structure		Name	Kinetic &Thermochemical	Comments
Decomposition starting from protonated INT2						
1	209	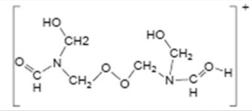	C6H13O6N2	INT2_P	Without barrier	INT2 + H$^+$ → INT2_P
2	179	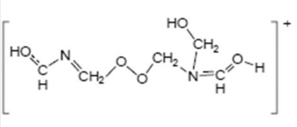	C5H11O5N2	INT3_P	ΔE$^\#$ =27.1 (29.7), ΔS$^\#$ = -6.8 ΔE$_{react}$ = 32.9 (29.6), ΔS$_{react}$ = 47.2 relative INT2_P	INT2_P → INT3_P+ H_2CO
3	88	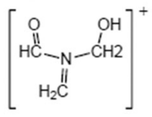	C3H6O2N	INT4_P	Without barrier ΔE = 22.8 (20.7), ΔS = 6.5 relative complex INT2_P	INT2 + H$^+$ → INT4_P + INT7
4	121	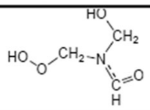	C3H7O4N	INT7		
5	45	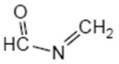	CH3ON	INT8	Without barrier	INT4_P + OH$^-$ → INT8 + H_2CO + H_2O
6	77	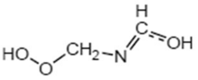	C2H5O3	INT9	ΔE$^\#$ =26.0 (27.8), ΔS$^\#$ = -0.4 ΔE$_{react}$ = 31.3 (29.5), ΔS$_{react}$ = 42.1 relative INT9	INT8 → INT9 + H_2CO
Decomposition starting from protonated INT6						
7	179	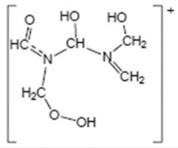	C5H11O5N2	INT6_P	Without barrier	INT6 + H$^+$ → INT6_P
8	120	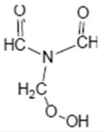	C3H6O4N	INT10	ΔE$^\#$ =13.4 (17.5), ΔS$^\#$ = 5.7 ΔE$_{react}$ = 8.5 (11.9), ΔS$_{react}$ = 17.3 relative INT11_P	INT6_P → INT10 + INT7_P
9	59	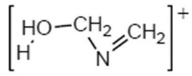	C2H5ON	INT7_P		
10	42	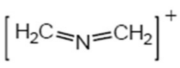	C2H4N	INT8_P	ΔE$^\#$ =1.4 (5.3), ΔS$^\#$ = -0.4 ΔE$_{react}$ = 3.4 (1.2), ΔS$_{react}$ = 34.6 relative INT9	INT7_P → INT8_P

be used instead of the more hazardous HMTD for canine and other vapor detection modes. It was observed that hexamine, substituted triazines, and linear amines are formed in the condensed phase, and the observation of these products is humidity dependant. The mechanism of formation of HMTD was found to proceed through a complete breakdown of hexamine, involving formaldehyde exchange. Positive identification of synthesis intermediates remains as a future work.

Acknowledgments

The authors thank the U. S. Department of Homeland Security and G-38 division of the US Army for funding of this work; however, the views contained herein are those of the authors only.

Table 10. Structure and properties of intermediate species observed during the decomposition of a HMTD-OH⁻ anion calculated using PBE0PBE1/cc-pVDZ level of theory. Energy values in kcal mol^{-1}, entropy values in cal K^{-1} mol^{-1}.

#	mass	structure		name	Kinetic &thermochemical	Reaction step and comments
1	225	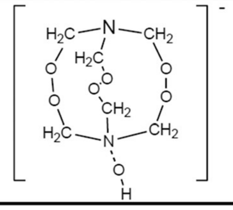	C6H13O7N2	INT1OH		HMTD +OH$^-$ → INT1OH
2	207	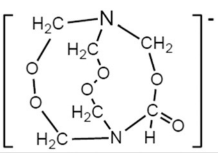	C6H11O6N2	INT2OH	$\Delta E^{\#}$ = -2.4 (-2.6), $\Delta S^{\#}$ = 3.8 ΔE_{react} = -108.2 (-104.9), ΔS_{react} = - 0.4 relative INT1OH	INT1OH → INT2OH + H_2O
3	207	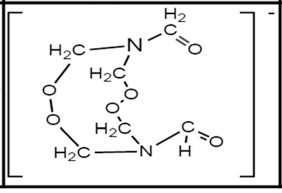	C6H11O6N2	INT3OH	$\Delta E^{\#}$ = 7.0 (4.9), $\Delta S^{\#}$ = 4.4 ΔE_{react} = 6.3 (4.3), ΔS_{react} = 9.6 relative INT2OH	INT2OH → INT3OH

References

[1] L. Legler, Über Produkte der langsamen Verbrennung des Aethyläthers, *Ber. Dtsch. Chem. Gesellsch.* **1885**, *18*, 3343.

[2] A. Baeyer, V. Villiger, Über die Nomenclatur der Superoxyde und die Superoxyde der Aldehyde, *Ber. Dtsch. Chem. Gesellsch.* **1900**, *33*, 2479.

[3] C. Von Girsewald, Beiträge zur Kenntnis des Wasserstoffperoxyds. Über die Einwirkung des Wasserstoffperoxyds auf Hexamethylentetramin, *Ber. Dtsch. Chem. Gesellsch.* **1912**, *45*, 2571.

[4] W. P. Schaefer, J. T. Fourkas, B. G. Tiemann, Structure of Hexamethylene Triperoxide Diamine, *J. Am. Chem. Soc.* **1985**, *107*, 2461.

[5] A. Wierzbicki, E. A. Salter, E. A Cioffi, E. D. Stevens, Density Functional Theory and X-ray Investigations of P- and M-Hexamethylene Triperoxide Diamine and Its Dialdehyde Derivative, *J. Phys. Chem. A* **2001**, *105*, 8763.

[6] J. C. Oxley, J. L. Smith, P. Bowden, R. Rettinger, Factors Influencing TATP and DADP Formation: Part I, *Propellants Explos. Pyrotech.* **2013**, *38*, 244.

[7] R. Matyas, J. Selesovsky, T. Musil, Decreasing the Friction Sensitivity of TATP, DADP, and HMTD, *Cent. Eur. J. Energ. Mater.* **2013**, *10*, 263.

[8] A. T. Nielsen, Structure and Chemistry of the Aldehyde Ammonias. 3. Formaldehyde-Ammonia Reaction. 1,3,5,-Hexahydrotriazine, *J. Org. Chem.* **1979**, *44*, 1678.

[9] N. Subramanian, *Method for Preparation of N-Phosphonomethylglycine*, US Patent US4422982A, Stauffer Chemical Company, Westport, CT, USA, **1983**.

[10] E. E. Gilbert, J. R. Leccacorvi, M. Warman, The Preparation of RDX from 1,3,5-Triacylhexahydro-s-triazines, *ACS Symp. Ser. (Ind. Lab. Nitrations Symp.)* **1976**, *22*, 327.

[11] A. Wexler, *Constant Humidity Solutions, CRC Handbook of Chemistry Physics* 85th ed, (Ed.: D. Lide), CRC Press, **2004**.

[12] K. Colizza, M. Porter, J. L. Smith, J. C. Oxley, Gas Phase Reactions of alcohols with hexamethylene triperoxide diamine (HMTD) under atmospheric pressure chemical ionization conditions, *Rapid Commun. Mass Spectrom.* **2015**, *29*, 74.

[13] J. C. Oxley, J. L. Smith, H. Chen, E. Cioffi, Decomposition of Multi-Peroxidic Compounds: Part II: Hexamethylene Triperoxide Diamine (HMTD), *Thermochim. Acta* **2002**, *38*, 215.

[14] J. Oxley, J. Zhang, J. Smith, E. Cioffi, Mass Spectra of Unlabeled and Isotopically Labeled Hexamethylene Triperoxide Diamine (HMTD), *Propellants Explos. Pyrotech.* **2000**, *25*, 1.

[15] J. C. Oxley, J. L. Smith, L. Lou, J. Brady, Determining Vapor Pressures of Diacetone Diperoxide (DADP) and Hexamethylene Triperoxide Diamine (HMTD), *Propellants Explos. Pyrotech.* **2009**, *34*, 539.

[16] J. C. Oxley, J. L. Smith, J. Brady, F. L.Steinkamp, Factors Influencing Destruction of Triacetone Triperoxide (TATP), *Propellants Explos. Pyrotech.* **2014**, *39*, 289.

[17] C. A. Taylor, W. Rinkenbach, HMTD, A New Detonating Explosive, *Army Ordnance* **1924**, *5*, 463; C. A. Taylor, W. Rinkenbach, Sensitivities of Detonating Compounds to Frictional Impact, Impact, and Heat, *J. Franklin Inst.* **1927**, *204*, 369.

[18] V. I. Siele, M. Warman, E. E. Gilbert, The Preparation of 3,7-Diacyl-1,3,5,7-tetraazabicylco[3.3.1]nonanes, *J. Heterocycl. Chem.* **1974**, *11*, 237.

[19] H. H. Richmond, G. S. Myers, G. F. Wright, The Reaction between Formaldehyde and Ammonia, *J. Am. Chem. Soc.* **1948**, *70*, 3659.

[20] L. Stefaniak, T. Urbanski, M. Witanowski, H. Januszewski, NMR Conformational Study of Cyclic Products from Degadation of Hexamethylenetetramine Hexahydro-1,3,5-triazines and Octahydro-1,3,5,7-Tetrazocines, *Roczniki Chemii Ann. Soc. Chim. Polonoru.* **1969**, *43*, 1687.

[21] W. E. Bachmann, J. C. Sheehan, A New Method of Preparing the High Explosives RDX, *J. Am. Chem. Soc.* **1949**, *71*, 1842.

[22] E. Aristoff, J. A. Graham, R. H. Meen, G. S. Myers, G. F. Wright, Nitrolysis of Hexamethylenetetramine, *Can. J. Res. B* **1949**, *27*, 520.

[23] J. M. Dreyfors, S. B. Jones, Y. Sayed, Hexamethylenetetramine: A Review, *Am. Ind. Hygiene Assoc. J.* **1989**, *50*, 579.

[24] C. M. Lock, H. Brust, M. van Breukelen, J. Dalmolen, M. Koeberg, D. A. Stoker, Investigation of Isotopic Linkages between Precursor Materials and the Improvised High Explosive Product Hexamethylene Triperoxide Diamine, *Anal. Chem.* **2012**, *84*, 4984.

[25] C. N. Satterfield, L. C. Case, Reaction of Aldehyde and Hydrogen Peroxide in Aqueous Solution, *Ind. Eng. Chem.* **1954**, *46*, 998; C. N. Satterfield, R. E. Wilson, R. M. LeClair, R. C. Reid, Analysis of Aqueous Mixtures of Hydrogen Peroxide and Aldehydes, *Anal. Chem.* **1954**, *26*, 1792.

[26] J. T. Edward, F. L. Chubb, D. F. R. Gilson, R. C. Hynes, F. Sauriol, A. Wiesenthal, Cage Peroxides have Planar Bridgehead Nitrogen Atoms, *Can. J. Chem.* **1999**, *77*, 1057.

Received: June 4, 2015
Revised: September 18, 2015